IEEE Access
Multidisciplinary ⋮ Rapid Review ⋮ Open Access Journal

Received 10 April 2025, accepted 1 May 2025, date of publication 5 May 2025, date of current version 14 May 2025.

Digital Object Identifier 10.1109/ACCESS.2025.3566948

RESEARCH ARTICLE

Wideband Circularly-Polarized Hexagonal SIW Cavity-Backed Slot Antenna With Enhanced Bandwidth and Compact Design

VAHID SARANI[1], ESRAA MOUSA ALI[2], MILAD SHARIATIFAR[3], BAL S. VIRDEE[4], (Senior Member, IEEE), DION MARIYANAYAGAM[4], NASR RASHID[5,6], MOHAMMAD ALIBAKHSHIKENARI[3,7], (Member, IEEE), AND MARIANA DALARSSON[8], (Senior Member, IEEE)

[1]Electrical Engineering Department, Ferdowsi University of Mashhad, Mashhad 9177948974, Iran
[2]Communications and Computer Engineering Department, Al-Ahliyya Amman University, Amman 19111, Jordan
[3]Electronics Engineering Department, University of Rome "Tor Vergata," 00133 Rome, Italy
[4]Center for Communications Technology, London Metropolitan University, N7 8DB London, U.K.
[5]Electrical Engineering Department, College of Engineering, Jouf University, Sakaka, Al Jowf 72388, Saudi Arabia
[6]Department of Electrical Engineering, Faculty of Engineering, Al-Azhar University, Nasr City, Cairo 11884, Egypt
[7]Department of Electrical and Electronics Engineering, Dogus University, 34775 Umraniye, Istanbul, Türkiye
[8]School of Electrical Engineering and Computer Science, KTH Royal Institute of Technology, 100 44 Stockholm, Sweden

Corresponding authors: Mohammad Alibakhshikenari (alibakhshikenari@ing.uniroma2.it) and Mariana Dalarsson (mardal@kth.se)

ABSTRACT This paper presents a novel wideband circularly polarized (CP) cavity-backed slot antenna based on Substrate Integrated Waveguide (SIW) technology, designed for compact and high-efficiency performance. The proposed antenna utilizes a hexagonal SIW cavity to simultaneously excite two closely spaced resonant modes (TM_{110} and TM_{210}), resulting in enhanced bandwidth for linear polarization (LP). To achieve circular polarization, a passive, single-layer linear-to-circular polarization converter is integrated above the cavity, offering a structurally simple and PCB-compatible solution. Unlike conventional CP designs that rely on complex feeding networks or multilayered structures, this configuration maintains a planar profile and efficient performance. A fabricated prototype demonstrates strong agreement between simulation and measurement, achieving a peak gain of 9.2 dBic and a 14% axial ratio (AR) bandwidth. These results highlight the antenna's suitability for modern wireless systems requiring wideband CP functionality, including satellite communications, 5G modules, and compact embedded devices.

INDEX TERMS Substrate integrated waveguide (SIW), broadband wireless access, hexagonal cavity, cavity backed slot antenna.

I. INTRODUCTION

Circularly polarized (CP) antennas are a cornerstone of contemporary wireless communication systems. Their unique ability to suppress polarization mismatches and mitigate multipath fading has made them indispensable in a wide range of applications, including satellite communications, radar systems, unmanned aerial vehicles (UAVs), and next-generation wireless networks [1], [2], [3], [4], [5]. Unlike linearly polarized (LP) antennas, CP antennas offer enhanced robustness in non-line-of-sight environments and provide more reliable communication links under dynamic orientation and mobility conditions.

Within this broad family of antennas, cavity-backed slot antennas have garnered significant attention due to their inherent advantages such as low profile, planar integration, and relatively simple fabrication. However, despite these strengths, a persistent limitation remains, narrow axial ratio (AR) bandwidth, which significantly constrains their ability to operate across wide frequency ranges without degradation in polarization purity [6]. This becomes especially problematic in broadband and high-data-rate communication systems that demand consistent performance over a wide spectral range [7], [8], [9].

The associate editor coordinating the review of this manuscript and approving it for publication was Wanchen Yang.

A substantial body of literature has attempted to improve the AR bandwidth of CP antennas using various structural and electromagnetic strategies. Some approaches rely on multi-feed configurations to excite orthogonal modes. For instance, the four-port array presented in [6] achieves a 10% AR bandwidth but introduces added complexity, increased size, and feed-network losses, factors that hinder miniaturization and integration.

Other studies employ hybrid structures such as Half-Mode SIW (HMSIW) and Quarter-Mode SIW (QMSIW) combined with patches or other resonators [10], [11], [12], [13]. While these designs offer compactness, they typically provide only limited AR bandwidth (1%–5%) and modest gain. Designs such as the QMSIW antenna in [14] require four coupled cavities and a central radiator to excite a single higher-order mode, achieving an AR bandwidth of 8.4% but at the expense of design complexity and size. Likewise, elliptic SIW cavities with dual-mode excitation, as in [15], achieve circular polarization via quasi-TM_{110} modes but attain only 1.63% AR bandwidth, which is insufficient for wideband applications.

In short, the critical issues in the existing literature include:

- Narrow AR bandwidth (typically $<10\%$) despite various enhancement techniques.
- Reliance on multi-port or multi-layer designs, which complicate fabrication and integration.
- Limited use of non-standard cavity geometries, such as hexagonal structures, for mode enhancement.
- Minimal demonstration of passive, single-layer polarization converters within SIW frameworks.

To address these gaps, this paper presents a novel wideband circularly polarized antenna based on a compact and efficient Substrate Integrated Waveguide (SIW) configuration. The proposed design introduces several technical innovations that differentiate it from prior art:

1. Unlike traditional rectangular or circular cavities, our antenna employs a hexagonal SIW cavity that enables simultaneous excitation of TM_{110} and TM_{210} modes using a non-resonant wide slot (NRWS), as illustrated in Fig. 1. This dual-mode excitation broadens the linear polarization (LP) bandwidth, serving as a solid foundation for wideband circular polarization. The specific use of the hexagonal cavity to engineer these hybrid resonances for CP performance is not found in the existing literature, marking a key novelty.
2. To achieve circular polarization without complex feed schemes or multiple substrate layers, a single-layer linear-to-circular polarization converter is placed at approximately half a guided wavelength ($\lambda g/2$) above the cavity. This converter consists of two diagonally oriented strip patches that generate orthogonal electric field components with a 90° phase difference thereby enabling efficient CP generation. This passive, low-profile approach eliminates the need for multilayer metasurfaces, stacked patches, or active circuits, making it both practical and manufacturable.
3. The proposed antenna achieves a 14% axial ratio bandwidth and a peak gain of 9.2 dBic both of which outperform comparable single-port designs in the literatures [11], [15], [16], and [17]. These metrics are accomplished while using a single-port feed, minimal layers, and thin substrates ($\lambda/42$), demonstrating exceptional performance without compromising compactness.
4. Unlike previous works that often trade off gain, bandwidth, or simplicity, this design optimally balances all three. It combines broad AR bandwidth, strong gain, and structural simplicity, positioning it as a strong candidate for integration into emerging systems such as IoT, UAVs, 5G modules, and compact satellite payloads.

This work directly addresses the shortcomings identified in the SIW CP antenna literature by introducing a novel hexagonal cavity geometry and a low-complexity polarization conversion strategy. It provides a clearly differentiated design that bridges the gap between performance and practicality, offering an efficient and manufacturable solution for modern wideband communication applications.

The remainder of this paper is organized as follows: Section II describes the antenna design, including the structure of the hexagonal cavity and the polarization conversion layer. Section III presents simulation and parametric analysis results. Section IV discusses fabrication and experimental validation. Section V provides a performance comparison with existing designs, and Section VI concludes the paper with key findings and directions for future research.

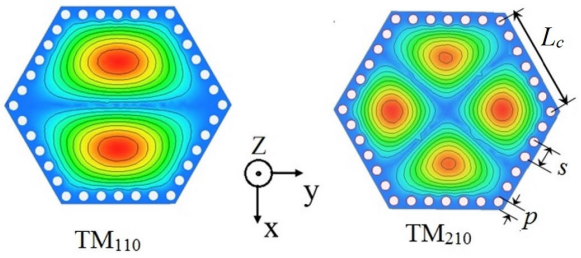

FIGURE 1. Simulated electric field distribution of the TE_{110} and TE_{210} modes of a hexagonal cavity ($L_c = 13.8$ mm).

II. ANTENNA DESIGN METHODOLOGY

A. LINEARLY POLARIZED ANTENNA

The proposed antenna is built upon a cavity-backed slot configuration designed to operate initially with linear polarization. At its core lies a hexagonal Substrate Integrated Waveguide cavity, which supports the excitation of TM_{110} and TM_{210} modes through a non-resonant wide slot (NRWS) etched onto its top surface. These two modes are closely spaced in frequency and, when simultaneously excited, contribute to enhanced impedance bandwidth and stable radiation performance.

While the hexagonal geometry may seem unconventional, it was deliberately selected after evaluating traditional SIW

cavity shapes such as rectangular, circular, and elliptical. Rectangular cavities, though easier to model and fabricate, typically exhibit more isolated modal behavior, which limits achievable AR bandwidth. Circular and elliptical cavities can support degenerate modes but generally require larger footprints and more complex designs to attain comparable bandwidth, and they tend to be more sensitive to fabrication tolerances.

In contrast, the hexagonal configuration offers a compact footprint and promotes a more uniform modal field distribution, enabling efficient dual-mode excitation (TM_{110} and TM_{210}) without increasing structural complexity. Importantly, it introduces no added fabrication difficulty, as it is fully compatible with standard PCB processes. This favorable combination of modal synergy, performance, and manufacturability was not observed to the same extent in conventional geometries during our preliminary analysis.

Importantly, the hexagonal cavity does not increase fabrication complexity. It is constructed using standard PCB milling and metallization techniques, without any need for curved walls, via transitions, or specialized substrates. As a result, the geometry offers an excellent balance between performance enhancement and manufacturability, justifying its selection over more conventional cavity shapes.

The proposed antenna geometry includes two radiating slots, with lengths L_{s1}, L_{s2} and widths W_{s1}, W_{s2}, symmetrically positioned at distances d_1 and d_2 from the center of the cavity, as shown in Fig. 2. A standard 50 Ω inset microstrip feed line excites the hexagonal cavity, efficiently stimulating both TE_{110} and TE_{210} modes to achieve wideband LP operation.

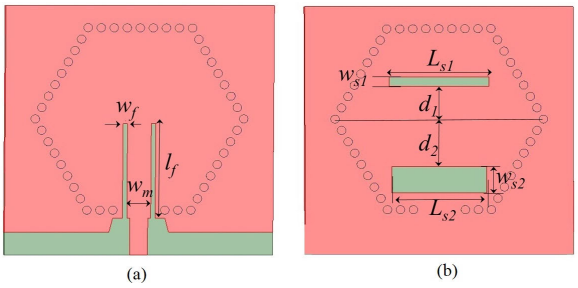

FIGURE 2. Fig. 2: The geometry of the LP cavity backed slot antenna, (a) top view, and (b) rear view. (L_c = 13.8 mm, l_f = 2.1 mm, w_f = 0.6 mm and w_{s1} = 1.4 mm).

The hexagonal cavity itself has a side length of 13.8 mm and is fabricated on a Rogers-Duroid 5880 substrate, characterized by a relative permittivity (ε_r) of 2.2, a thickness of 0.787 mm, and a loss tangent of 0.0009. Measurement results, detailed in Section IV, confirm that the LP antenna achieves an impedance bandwidth of 14% and a peak gain of 7.6 dBi, validating the effectiveness of the dual-mode excitation within this compact structure.

The design of the proposed antenna followed a structured and iterative process, outlined as follows:

1. *Cavity Shape Selection*: Begin with a comparative study of conventional SIW cavity shapes (rectangular, circular, elliptical) and select the hexagonal geometry based on its ability to support dual-mode excitation (TM_{110} and TM_{210}) within a compact footprint.
2. *Initial Slot Configuration*: Place two non-resonant wide slots on the top surface of the hexagonal cavity and use parametric sweeps to adjust their lengths (*Ls1*, *Ls2*) and widths (*Ws1*, *Ws2*) for optimal impedance matching.
3. *Feed Design*: Design and tune a 50 Ω inset microstrip feed line to excite the cavity effectively, targeting simultaneous excitation of the two modes.
4. *LP Bandwidth Optimization*: Use full-wave simulations to optimize cavity dimensions and slot parameters to maximize LP bandwidth.
5. *Polarization Converter Integration*: Design a single-layer slanted-strip converter placed at a separation distance of *h_mid* ≈ λg/2, and tune strip dimensions and spacing to enable orthogonal field components with a 90° phase difference.
6. *Parametric Fine-Tuning*: Conduct a series of parametric studies on key variables (slot position, strip length/width, separation distance) to maximize AR bandwidth and gain.
7. *Fabrication and Measurement*: Finalize the optimized geometry and fabricate a prototype using standard PCB processes. Measure S_{11}, AR, gain, and radiation patterns for experimental validation.

It is worth noting that although air-filled SIW structures are known to offer advantages in terms of reduced dielectric loss and potentially increased bandwidth, they were intentionally not adopted in this design. Air-filled SIWs typically require more complex fabrication procedures, such as precision mechanical support or bonding steps to maintain the air gap, which increase production cost and reduce structural robustness. In contrast, the use of a substrate-filled SIW allows for fully planar, low-profile fabrication using standard PCB processes, which is ideal for scalable and cost-effective deployment. Furthermore, despite the slightly higher dielectric loss, the proposed antenna demonstrates excellent performance, achieving a 14% impedance bandwidth and 9.2 dBic gain metrics that are competitive even against some air-filled implementations. Thus, the design trade-off favors practicality, mechanical stability, and integration ease without significantly compromising electromagnetic performance.

B. CIRCULARLY POLARIZED ANTENNA

To enable circular polarization, a single-layer passive polarization converter is introduced above the linearly polarized antenna. This converter comprises two slanted metallic strips, each approximately λg/2 in length, etched onto a 0.5 mm-thick Rogers 5880 substrate. Positioned at a height *h_mid* roughly half a guided wavelength above the radiating slot the converter is excited by the field radiated from the underlying cavity-backed structure.

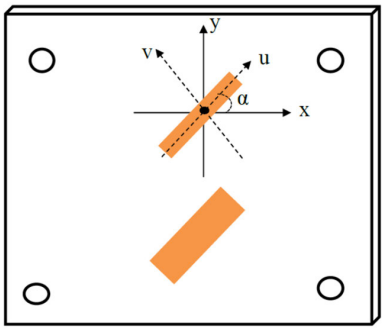

FIGURE 3. Linear to circular polarization converter model.

As illustrated in Fig. 3, the slanted strips serve as a polarizing surface, generating two orthogonal electric field components: one aligned with the strip orientation and the other perpendicular to it. By carefully tuning the strip dimensions, spacing, and placement relative to the source, these components are excited with a 90° phase difference, effectively transforming the linearly polarized wave into a circularly polarized one [18], [19].

Although the inclusion of this additional layer may appear to introduce complexity, the overall design remains structurally simple and highly manufacturable. The converter:

- Does not require vias, multi-port feeds, or active tuning components.
- Involves no complex alignment or bonding processes.
- Can be produced using standard PCB fabrication techniques, ensuring suitability for low-cost and scalable implementation.

This design approach is therefore justified not only by its fabrication practicality but also by its demonstrated performance advantages. Specifically, the integration of the polarization converter results in a 14% AR bandwidth and a peak gain of 9.2 dBic, both of which exceed the capabilities of many comparable CP antennas reported in the literature. This efficient yet simple configuration makes the proposed design a strong candidate for integration into modern wireless systems that demand compactness, performance, and manufacturability.

As shown in Fig. 3, the linear-to-circular polarization converter employs a structure symmetric along the $u - v$ coordinates. This symmetry eliminates cross-polarized transmitted components, ensuring that the transmitted electric field (E-field) maintains consistent polarization properties. The mathematical relationship between the incident and transmitted waves is expressed using a transmission matrix, as shown in Equation (1) [3]:

$$\begin{bmatrix} E_u^t \\ E_v^t \end{bmatrix} = \begin{bmatrix} t_{uu} & 0 \\ 0 & t_{vv} \end{bmatrix} \begin{bmatrix} E_u^i \\ E_v^i \end{bmatrix} \tag{1}$$

Here, E^t and E^i are transmitted and incident waves respectively, while parameters t_{uu} and t_{vv} are transmission matrix coefficients that describe the behavior of the converter for each polarization component. If the incident wave is linearly y-polarized, it can be expressed as:

$$E^i = E_0 \vec{a}_y \tag{2}$$

When the angle of incidence $\alpha = 45^{\text{o}}$, the wave is decomposed into components along the u-v coordinates, and the incident wave can be rewritten as:

$$E^i = E_0 \cos\left(45^o\right)\left(\vec{a}_u + \vec{a}_v\right) \tag{3}$$

Based on the transmission matrix of Equations (1) and the decomposition in Equation (3), the transmitted wave can be expressed as:

$$\begin{aligned} E^t &= E_u^t + E_v^t = t_{uu}E_u^i + t_{vv}E_v^i \\ E^t &= E_0 cos(45^0)\left(t_{uu}\vec{a}_u + t_{vv}\vec{a}_v\right) \end{aligned} \tag{4}$$

As shown in Equation (4), the polarization of the transmitted wave depends on the magnitude and phase of parameters t_{uu} and t_{vv}. The phase difference is expressed as:

$$\Delta\emptyset_{vu} = Arg\left(t_{vv}\right) - Arg\left(t_{uu}\right) \tag{5}$$

Plays a crucial role in determining the resulting polarization.

For the transmitted wave to achieve circular polarization, two conditions must be satisfied within the operating frequency range:

1. $|t_{uu}| = |t_{vv}|$
2. $\Delta\emptyset_{vu} \approx \pm 90^0$, ensuring the required phase shift for circular polarization.

When these conditions are met, the transmitted wave exhibits circular polarization over the desired frequency band.

The axial ratio of the transmitted wave, a critical metric for circular polarization, is defined by Equation (6) [20].

$$\begin{aligned} AR &= \left(\frac{|t_{uu}|^2 + |t_{vv}|^2 + \sqrt{a}}{|t_{uu}|^2 + |t_{vv}|^2 - \sqrt{a}}\right)^{1/2} \\ a &= |t_{uu}|^4 + |t_{vv}|^4 + 2\,|t_{uu}|^2\,|t_{vv}|^2 \cos\left(2\Delta\emptyset_{vu}\right) \end{aligned} \tag{6}$$

The AR quantifies the degree of polarization, with a value close to 1 indicating ideal circular polarization. By fine-tuning the transmission coefficients (t_{uu}, t_{vv}) and ensuring the appropriate phase difference ($\Delta\phi_{\text{vu}}$), the design achieves an optimal AR, confirming the converter's efficiency in generating circularly polarized waves.

The proposed polarization converter design is highly efficient due to its symmetric structure and simple configuration. By carefully adjusting the slant angle α, the geometry of the converter, and the transmission coefficients, the design ensures robust circular polarization over a wide bandwidth. This approach is particularly advantageous for applications requiring compact, efficient, and high-performance CP antennas, such as satellite communication and IoT devices.

III. PARAMETERIC INVESTIGATION

To evaluate the radiation performance of the proposed antenna shown in Fig. 4, a parametric study is conducted to analyze the effects of the strip patch on impedance and AR bandwidth.

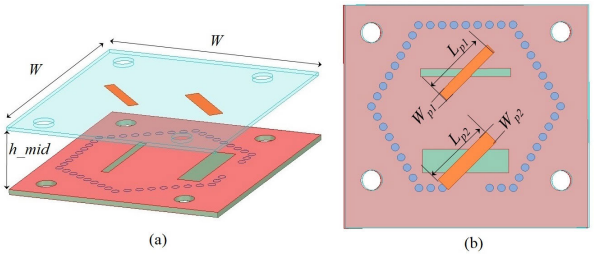

FIGURE 4. The geometrical configuration of the proposed CP wideband antenna, (a) perspective view, and (b) top view of both top and bottom layers.

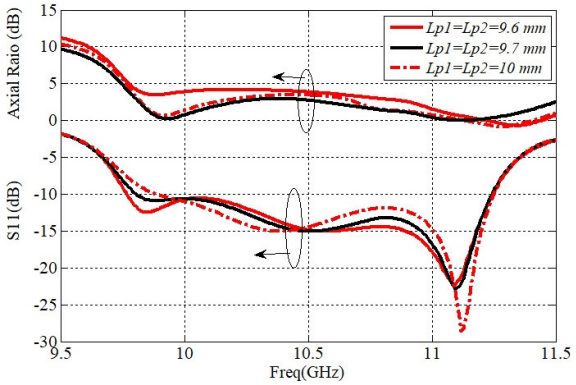

FIGURE 5. The effect of the length of strip patches for $W_{p1} = 1.5$ mm and $W_{p2} =$ mm on S_{11} and AR of the CP antenna.

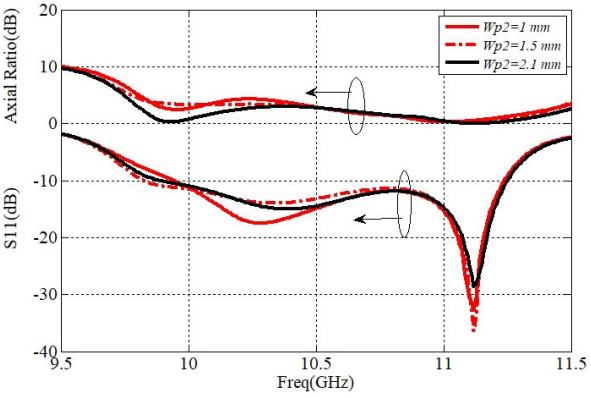

FIGURE 6. The effect of width of patches for $L_{p1} = L_{p2} = 10$ mm on S_{11} and *AR* of the proposed circularly polarized antenna.

A. EFFECT OF THE STRIP DIMENSIONS

The initial lengths of both strips are set to approximately half the free-space wavelength at the center frequency. These values are then fine-tuned around the initial estimates, and the antenna is simulated using HFSS software to optimize impedance and AR bandwidth. The simulated S_{11} and AR results are shown in Fig. 5 and Fig. 6 as functions of frequency. It is observed that for $W_{p1} = 1.5$ mm and $W_{p2} = 2.1$, the AR bandwidth is significantly improved, extending from 9.9 GHz to 11.25 GHz when $L_{p1} = L_{p2} = 10$ mm.

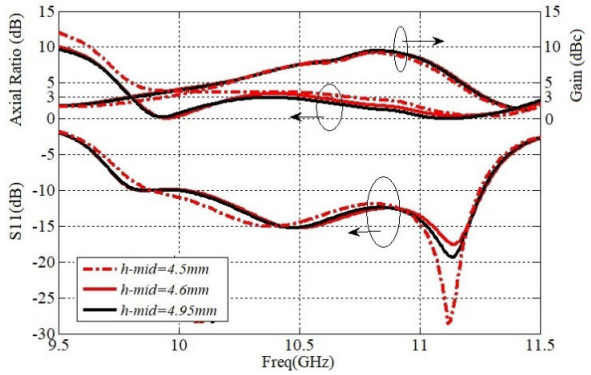

FIGURE 7. The effect of the distance between two layers on S_{11}, AR and gain of the proposed circularly polarized antenna.

TABLE 1. The geometrical parameters of the proposed antenna.

Parameter	Dimension (mm)	Parameter	Dimension (mm)
L_{s1}	12.75	d_x	0.40
L_{s2}	12.75	d_c	27.60
Ws_1	1.40	w_m	3.19
W_{s2}	3.50	W_1	34.30
L_c	13.80	W_2	33.30
d_1	5	p	1
d_2	8.05	s	1.50
l_f	12.90	W_{p1}	1.50
w_f	0.60	W_{p2}	2.10
L_{p1}	10	h_mid	4.95
L_{p2}	9.97		

B. EFFECT OF THE DISTANCE BETWEEN SLOTS AND POLARIZED CONVERTOR

Two 45° inclined patches are applied to each slot to generate a circularly polarized wave. To optimize the AR and gain, a parametric study is conducted to analyze the effects of the distance between the patches and the slots *h_mid* on S_{11} and AR. The results, presented in Fig. 7, confirm that by adjusting *h_mid*, an optimal AR bandwidth can be achieved.

IV. MEASURED RESULTS AND DISCUSSION

Fig. 8 shows the fabricated dual-layer proposed CP antenna, with the adjusted geometrical parameters listed in Table 1. The measured S_{11}, axial ratio, and antenna gain as functions of frequency are presented in Fig. 9 and Fig. 10, showing good agreement between simulation and measurement results. The measured 3 dB AR and 3 dB gain bandwidth range from 9.8 GHz to 11.3 GHz, providing a fractional bandwidth of 14%. The antenna achieves a maximum gain of 9.15 dBic at 10.8 GHz.

Fig. 11 shows the simulated and measured normalized radiation patterns for the standard E- and H-planes. The proposed antenna demonstrates broadside radiation patterns with suitable gain across the operating bandwidth. As shown in Fig. 11, the antenna radiates right-hand circularly polarized (RHCP) waves at 9.8 GHz, 10.5 GHz, 10.85 GHz, and 11.1 GHz. The measured left-hand circularly polarized (LHCP) levels are below −18 dB in both $\phi = 0°$ and

TABLE 2. Performance comparison with existing CP antennas.

Ref.	Technique	No. of Ports	Freq (GHz)	AR BW (%)	Gain (dBic)	Total Height (mm / λ_0)	Polarization	Size (λ_o^2)
[6]	4-Port Patch Array	4	30	10	12.5	11.2 / 0.392	RHCP	0.70×0.70
[12]	HMSIW + Patch	1	9.5	5	6.8	6.0 / 0.21	LHCP	0.64×0.75
[15]	Elliptic SIW Cavity	1	12.24	1.63	8.1	7.2 / 0.25	LHCP	0.92×0.90
[16]	2-Port SIW Cavity	2	9.5	12	7.6	8.1 / 0.28	RHCP	1.30×1.30
[17]	Single-Port Cavity	1	5.8	0.7	7.4	6.5 / 0.23	RHCP	1.30×1.30
This Work	Hexagonal SIW + Converter	1	10.5	14	9.2	6.237 / 0.218	RHCP	0.66×0.79

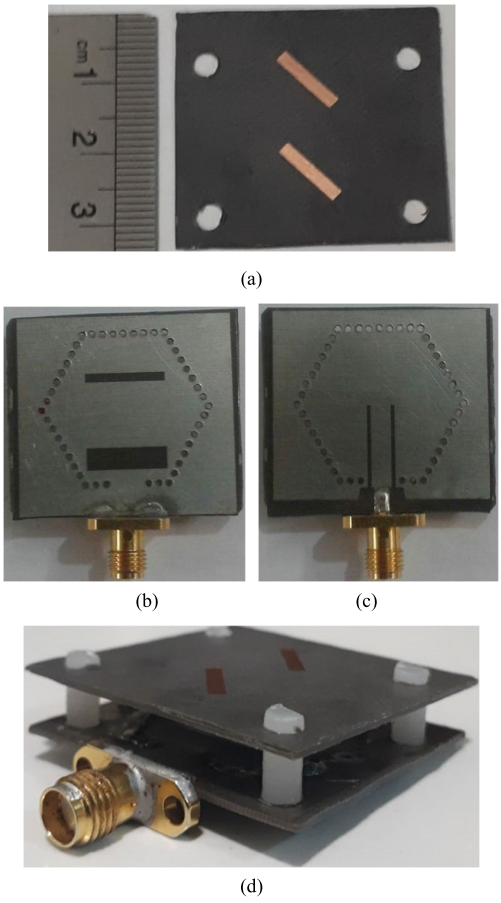

FIGURE 8. The fabricated prototype of the proposed antenna, (a) top-view of the top-layer, (b) top-view of the bottom-layer, and (c) back-view of the bottom-layer, (d) assembled antenna structure.

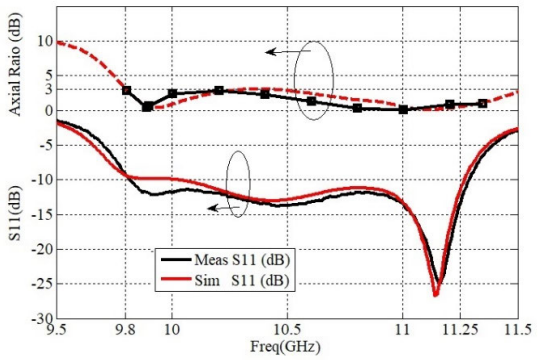

FIGURE 9. The simulated and measured S_{11} and AR for single antenna.

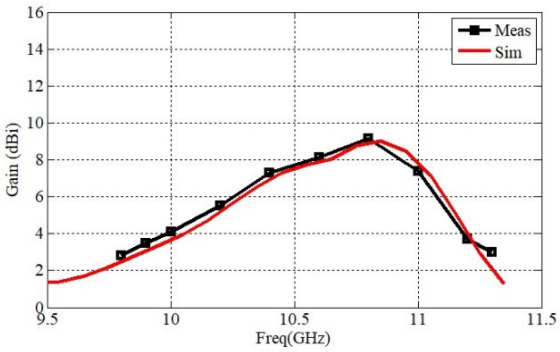

FIGURE 10. The simulated and measured gain of the proposed antenna.

90° standard planes, except at 9.8 GHz, where the LHCP level is −15 dB.

The differences observed between RHCP and LHCP components at $\theta = 0°$ in both $\phi = 0°$ and $\phi = 90°$ planes, particularly at 9.8 GHz and 10.5 GHz, stem from the frequency-dependent behavior of the linear-to-circular polarization converter. At 9.8 GHz, the lower edge of the axial-ratio bandwidth, the polarization conversion is not fully optimized, resulting in slightly higher LHCP leakage. At 10.5 GHz, the imbalance may arise from fabrication tolerances and slight misalignments, which become more prominent near the band center where field coupling is strongest. Despite these minor variations, the RHCP remains dominant across the operational band, with LHCP levels generally below −18 dB, confirming the overall effectiveness of the CP radiation. These effects are within expected behavior for wideband CP antennas employing passive converters and do not compromise the antenna's practical performance.

V. COMPARATIVE STUDY

The radiation performance of the proposed wideband circularly polarized antenna is benchmarked against recent state-of-the-art CP designs, as summarized in Table 2. The proposed antenna achieves a broad axial ratio bandwidth of 14% and a peak gain of 9.2 dBic, using a compact, single-feed architecture. Its structure consists of a hexagonal SIW cavity and a passive single-layer polarization converter, both fabricated using standard PCB techniques.

Compared to the 4-port patch array in [6], which achieves a 10% AR bandwidth and 12.5 dBic gain at 30 GHz, the proposed design offers similar polarization performance with

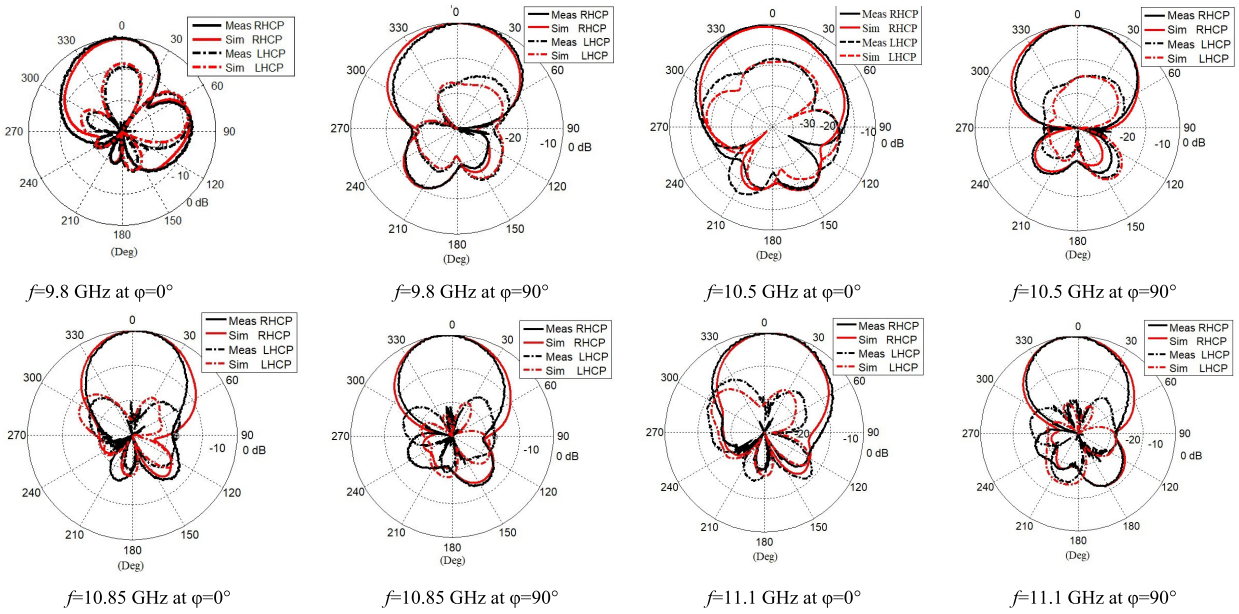

FIGURE 11. The measured and simulated radiation patterns of the proposed CP antenna.

a significantly simpler feed network. The multi-port configuration in [6] introduces feed complexity, higher insertion loss, and increased design cost, challenges avoided in the single-port configuration presented here.

Hybrid SIW designs such as the HMSIW + patch structure in [12] demonstrate modest improvements in bandwidth, achieving 5% AR bandwidth and 6.8 dBic gain. However, these designs require hybrid substrate structures and additional tuning, which reduce manufacturing simplicity. The elliptic SIW cavity antenna in [15] achieves 1.63% AR bandwidth and 8.1 dBic gain but still underperforms in terms of bandwidth due to limited modal diversity. The proposed antenna, by contrast, leverages two distinct TM modes (TM_{110} and TM_{210}) in a hexagonal cavity, yielding a broader operational band.

The two-port SIW cavity design in [16] offers 12% AR bandwidth and 7.6 dBic gain, yet its dual-port structure requires careful isolation and feed balancing, which add complexity to the system. The single-port cavity design in [17] provides only 0.7% AR bandwidth and 7.4 dBic gain, demonstrating the limitations of single-mode SIW cavities when not supported by a polarization converter.

A critical parameter often overlooked in earlier works is total antenna height. Many prior comparisons cite only substrate thickness, which does not accurately reflect the overall profile of an antenna in real-world implementations. In this work, we report a total antenna height of 6.237 mm, corresponding to 0.218λ at 10.5 GHz. This includes the base substrate (0.787 mm), air gap (4.95 mm), and the converter layer (0.5 mm). Compared to the total heights of 11.2 mm in [6], 8.1 mm in [16], and 7.2 mm in [15], the proposed antenna offers a compact profile without sacrificing gain or bandwidth. While not the lowest profile in absolute terms, the proposed design maintains a practical form factor and is compatible with low-profile systems due to its entirely planar construction and use of PCB materials.

Alternative CP antenna technologies, such as dielectric resonator antennas (DRAs) and metasurface-based structures, can also achieve wideband operation. However, these approaches typically involve greater fabrication complexity. DRAs often require custom ceramic materials, 3D machining, and precise alignment. Metasurface-based antennas rely on subwavelength patterning and multilayer structures, which increase cost and sensitivity to fabrication tolerances. In contrast, the proposed antenna is fully compatible with low-cost, mass-producible PCB fabrication processes and offers a favorable trade-off between gain, bandwidth, profile, and complexity.

The proposed antenna outperforms many existing designs in terms of AR bandwidth and gain while maintaining structural simplicity and a moderate height. It avoids multi-port feeding and complex three-dimensional elements, resulting in a circularly polarized antenna that is efficient, compact, and well-suited for practical deployment in modern communication systems such as 5G, satellite links, UAVs, and IoT terminals.

VI. CONCLUSION

This paper presents a compact and efficient circularly polarized (CP) antenna based on a hexagonal SIW cavity-backed slot design. The antenna leverages dual-mode excitation (TM_{110} and TM_{210}) within a novel hexagonal cavity structure to achieve wide linear polarization bandwidth. A passive, single-layer polarization converter, comprising two diagonally oriented slant strips, is introduced to enable wideband circular polarization.

While this converter introduces an additional layer, it adds minimal complexity, requires no active components or

complex feeds, and is easily fabricated using standard PCB techniques. This design strategy offers a practical trade-off: significantly enhanced performance in terms of AR bandwidth (14%) and gain (9.2 dBic) with minimal manufacturing and design overhead. It eliminates the need for multi-port excitation or multilayer stacked configurations that typically complicate implementation and increase cost.

In addition, although air-filled SIW structures are known to offer lower loss and potentially higher bandwidth, they often require specialized fabrication techniques and increased mechanical complexity, which are not suitable for low-profile, mass-produced systems. The use of substrate-filled SIW in this work ensures mechanical stability, ease of manufacturing, and integration compatibility, while still achieving competitive performance metrics. This design choice reinforces the antenna's viability for scalable applications in cost-sensitive and compact environments.

Compared to prior works, the proposed antenna achieves superior performance with a simpler, low-profile, and manufacturable architecture, making it ideal for real-world applications such as satellite communications, UAVs, 5G modules, and IoT devices. The findings of this study demonstrate the potential of integrating mode-engineered SIW cavities with compact passive polarization conversion layers to realize high-performance CP antennas in space- and cost-constrained environments.

REFERENCES

[1] J.-D. Zhang, L. Zhu, N.-W. Liu, and W. Wu, "Dual-band and dual-circularly polarized single-layer microstrip array based on multiresonant modes," *IEEE Trans. Antennas Propag.*, vol. 65, no. 3, pp. 1428–1433, Mar. 2017.

[2] M. Fazaelifar, S. Jam, and R. Basiri, "A circular polarized reflectarray antenna with electronically steerable beam and interchangeable polarizations," *Int. J. Microw. Wireless Technol.*, vol. 13, no. 2, pp. 198–210, Mar. 2021.

[3] F. Sadeghikia, M. Valipour, M. T. Noghani, H. Ja'afar, and A. K. Horestani, "3D beam steering end-fire helical antenna with beamwidth control using plasma reflectors," *IEEE Trans. Antennas Propag.*, vol. 69, no. 5, pp. 2507–2512, May 2021.

[4] N. Qasem, "Measurement and simulation for improving indoor wireless communication system performance at 2.4 GHz by modifying the environment," *IEEE Access*, vol. 12, pp. 96660–96671, 2024.

[5] M. Z. Iskandarani, "Investigation of energy consumption in WSNs within enclosed spaces using beamforming and LMS (BF-LMS)," *IEEE Access*, vol. 12, pp. 63932–63941, 2024.

[6] S. Mener, R. Gillard, and L. Roy, "A dual-band dual-circular-polarization antenna for Ka-band satellite communications," *IEEE Antennas Wireless Propag. Lett.*, vol. 16, pp. 274–277, 2017.

[7] A. M. Etman, M. S. Abdalzaher, A. A. Emran, A. Yahya, and M. Shaaban, "A survey on machine learning techniques in smart grids based on wireless sensor networks," *IEEE Access*, vol. 13, pp. 2604–2627, 2025.

[8] Z. H. Tantawy, M. B. El Mashade, A. A. Emran, and A. I. M. Semeia, "On the performance of FSO communication system with WDM and MIMO structure under different turbulent atmospheric conditions," *J. Opt. Commun.*, vol. 45, no. s1, pp. s2133–s2149, Jan. 2025.

[9] M. Elsharief, A. A. Emran, H. Hassan, S. R. Sabuj, and H.-S. Jo, "SLES: Scheduling-based low energy synchronization for industrial Internet of Things," *IEEE Sensors J.*, vol. 22, no. 16, pp. 16652–16661, Aug. 2022.

[10] H. Dashti and M. H. Neshati, "Development of low-profile patch and semi-circular SIW cavity hybrid antennas," *IEEE Trans. Antennas Propag.*, vol. 62, no. 9, pp. 4481–4488, Sep. 2014.

[11] S. A. Razavi and M. H. Neshati, "Development of a low-profile circularly polarized cavity-backed antenna using HMSIW technique," *IEEE Trans. Antennas Propag.*, vol. 61, no. 3, pp. 1041–1047, Mar. 2013.

[12] A. Vahid Sarani and M. H. Neshati, "Design investigation of dual-band dual-circularly polarized hybrid antenna array using semi-hexagonal HMSIW cavity," *AEU-Int. J. Electron. Commun.*, vol. 157, Dec. 2022, Art. no. 154437.

[13] A. V. Sarani and M. H. Neshati, "Development of a dual band circularly polarized mircostrip patch and semi-hexagonal SIW cavity hybrid antenna," in *Proc. 23rd Iranian Conf. Electr. Eng.*, Tehran, Iran, May 2015, pp. 329–332, doi: 10.1109/IranianCEE.2015.7146234.

[14] C. Jin, Z. Shen, R. Li, and A. Alphones, "Compact circularly polarized antenna based on quarter-mode substrate integrated waveguide sub-array," *IEEE Trans. Antennas Propag.*, vol. 62, no. 2, pp. 963–967, Feb. 2014.

[15] Y. Xu, Z. Wang, and Y. Dong, "Circularly polarized slot antennas with dual-mode elliptic cavity," *IEEE Antennas Wireless Propag. Lett.*, vol. 19, pp. 715–719, 2020.

[16] W. Wang, H. Jin, W. Yu, X. H. Zhang, F. Wu, K.-S. Chin, and G. Q. Luo, "A single-layer dual-circularly polarized SIW-cavity-backed patch filtenna with wide axial-ratio bandwidth," *IEEE Antennas Wireless Propag. Lett.*, vol. 20, no. 6, pp. 908–912, Jun. 2021.

[17] T. Yang, Z. Zhao, D. Yang, and Z. Nie, "A single-layer circularly polarized antenna with improved gain based on quarter-mode substrate integrated waveguide cavities array," *IEEE Antennas Wireless Propag. Lett.*, vol. 19, no. 12, pp. 2388–2392, Dec. 2020.

[18] K.-S. Min, J. Hirokawa, K. Sakurai, M. Ando, and N. Goto, "Single-layer dipole array for linear-to-circular polarisation conversion of slotted waveguide array," *IEE Proc.-Microw., Antennas Propag.*, vol. 143, no. 3, pp. 211–216, Jun. 1996.

[19] W. Ma, W. Cao, S. Shi, and X. Yang, "Compact high gain leaky-wave antennas based on substrate integrated waveguide TE_{220} mode," *IEEE Access*, vol. 7, pp. 145060–145066, 2019.

[20] B. Lin, J. Guo, Y. Ma, W. Wu, X. Duan, Z. Wang, and Y. Li, "Design of a wideband transmissive linear-to-circular polarization converter based on a metasurface," *Appl. Phys. A, Solids Surf.*, vol. 124, no. 10, p. 715, Oct. 2018, doi: 10.1007/s00339-018-2135-y.

VAHID SARANI was born in Zabol, Iran. He received the M.Sc. degree in communication engineering from the Ferdowsi University of Mashhad, Iran. His current research interests include antenna designs and measurements.

ESRAA MOUSA ALI received the B.Sc. degree in electrical and computer engineering from Hashemite University, in 2010, the M.Sc. degree in electrical and electronic engineering from University Sains Malaysia (USM), in 2013, and the Ph.D. degree in electrical and electronic engineering from University Technology PETRONAS (UTP), in 2019. She is currently an Associate Professor with Al-Ahliyya Amman University, where she is with the Faculty of Engineering. She published more than 40 research papers in peer-reviewed journals and conference proceedings.

MILAD SHARIATIFAR received the Ph.D. degree in electronic and communication engineering from the Shahed University of Tehran, Iran. He is currently a Senior Researcher with the University of Rome "Tor Vergata," Italy. He was a Postdoctoral Researcher with Instituto de Telecomunicações, Aveiro, Portugal, and the University of Amirkabir, Tehran, Iran. His main research interests include the design of microwave circuits, especially power amplifier theory, design, efficiency improvement, and linearization techniques. He has been a reviewer of several IEEE transactions and other journal articles.

BAL S. VIRDEE (Senior Member, IEEE) received the B.Sc. and M.Phil. degrees in communications engineering from the University of Leeds, U.K., and the Ph.D. degree in electronic engineering from the University of London, U.K. He has worked in industry for various companies including Philips (U.K.) as a Research and Development-Engineer and Teledyne Defence and Space as a Future Products Developer in RF/microwave communications. He has taught at several academic institutions before joining London Metropolitan University, where he is currently a Senior Professor of communications technology with the School of Computing and Digital Media, where he is the Head of the Communications Technology Research Center. His research, in collaboration with industry and academia, is in wireless communications encompassing mobile phones to satellite technology. He has chaired technical sessions at IEEE international conferences and published numerous research papers. He is an Executive Member of IET's Technical and Professional Network Committee on RF/Microwave Technology. He is a fellow of IET.

DION MARIYANAYAGAM received the B.Eng. degree (Hons.) in computer systems engineering from London Metropolitan University. Over the years, he has amassed a wealth of experience, having been a Consultant for a range of technology companies and startups across the U.K. Currently, he is a Senior Lecturer with London Metropolitan University while continuing his role as a Consultant. He is an accomplished professional and academic in the field of technology. His expertise spans several cutting-edge areas of technology. His work bridges the gap between academia and industry, driving innovation, and contributing to technological progress. His research interests include advancing communications technology, ensuring robust security systems, and exploring the applications of sensors, the Internet of Things (IoT), and robotics.

NASR RASHID was born in Egypt, in 1973. He received the B.Sc. (Hons.), M.Sc., and Ph.D. degrees in electronics and communication engineering from Al-Azhar University, Cairo, Egypt, in 1996, 2004, and 2009, respectively. He is currently an Assistant Professor with the Department of Electrical Engineering, College of Engineering, Jouf University, Sakaka, Saudi Arabia. His research interests include wireless communications, antennas and wave propagations, multiple-input multiple-output (MIMO) systems, impedance-matching circuits, microwave components, and gap waveguide technology.

MOHAMMAD ALIBAKHSHIKENARI (Member, IEEE) was born in Mazandaran, Iran, in February 1988. He received the Ph.D. degree (cum laude) in electronics engineering from the University of Rome "Tor Vergata," (UNITOV), Italy, in February 2020. From May to December 2018, he was a Ph.D. Visiting Researcher with the Chalmers University of Technology, Gothenburg, Sweden. His training during this visit included a research stage at Swedish Company "Gap Waves AB." From November 2016 to February 2020, during the Ph.D. degree, he attended 13 European Ph.D. schools in the fields of electromagnetics, antennas, metamaterials, metasurfaces, RF and microwave technologies, millimeter-waves and terahertz circuits, which were organized by various European universities and organizations, and he successfully achieved all the credits leading him to obtain the Ph.D. degree with a European label. In November 2019, he was a winner of a Postdoctoral Research Fund for two years awarded by UNITOV. From July 2021 to August 2024, he was with the Department of Signal Theory and Communications, Universidad Carlos III de Madrid (UC3M), Spain, as a Principal Investigator of the CONnecting EXcellence (CONEX)-Plus Talent Training Program and Marie Skodowska-Curie Actions. During this Program, he has spent two secondments at the: 1) Microwave Engineering Center for Space Applications (MECSA), Rome, Italy , from April to August 2024; and 2) SARAS Technology Ltd., Company, Leeds, U.K., from December 2022 to May 2023. In addition, during this program he had some short research visits at the: 1) University of Catania, Italy, in May 2024, along with an invited lecture titled "Terahertz Antennas based on Metasurface and SIW" for the master's and Ph.D. students, and postdoctoral researchers; 2) University of Messina, Italy, in May 2024; 3) University of Bradford, U.K., in May 2023; and 4) Edinburgh Napier University, U.K., in April 2023. In 2021 and 2022, he received the "Teaching Excellent Acknowledgement" certificate for the course of "electromagnetic fields" from the Vice-Rector of Studies of UC3M. In September 2024, he joined UNITOV, as a Senior Researcher. His research interests include electromagnetic systems, antennas and wave-propagations, metamaterials and metasurfaces, RF and microwave technologies, sensors, synthetic aperture radars (SAR), 5G and beyond wireless communications, multiple input multiple output (MIMO) systems, RFID tag antennas, substrate integrated waveguides (SIWs), impedance matching circuits, millimeter-waves and terahertz integrated circuits, gap waveguide technology, beamforming networks, and reconfigurable intelligent surfaces (RIS)," leading him to publish one book, nine book chapters, more than 150 research articles in scientific journals, and more than 100 research papers in international conferences, including 47 in-person presentations in 29 conferences and 26 on-line presentations in 12 conferences. His research works received more than 7700 citations with an H-index above 54 reported by Scopus, Google Scholar, and ResearchGate. According to Stanford University's yearly analysis, he has been among the World's Top 2% Scientists of highly cited scientific authors, since 2020. He was listed in both Career Long and Single Year Impact in Stanford's list. He was a recipient of the two young engineer awards of the 47th and 48th European Microwave Conferences held in Nuremberg, Germany, in 2017, and Madrid, Spain, in 2018, respectively. In April 2020, his research article titled "High-Gain Metasurface in Polyimide On-Chip Antenna Based on CRLH-TL for Sub Terahertz Integrated Circuits, Scientific Reports, volume ten, Article number 4298, in 2020" was awarded as the Best Month Paper at the University of Bradford, U.K. In addition, he serves the role of an Associate Editor for two scientific journals of *Radio Science* and *The Journal of Engineering* (IET). He acts as a referee in several journals, the technical program committee (TPC), and the session chair of several international conferences. In addition, he is a member of the reviewer panel of the Dutch Research Council (NWO) and U.K. Research and Innovation (UKRI) Funding Service and the External Examiner of several Ph.D. dissertations from various worldwide universities.

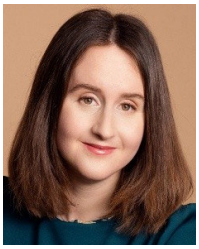

MARIANA DALARSSON (Senior Member, IEEE) received the M.Sc. degree in physics and Ph.D. degree in electromagnetic theory from the KTH Royal Institute of Technology, Stockholm, Sweden, in 2010 and 2016, respectively, and the Docent degree from the Group of Waves, Signals, and Systems, Linnaeus University, Växjö, Sweden, in 2019. From 2016 to 2019, she was a Postdoctoral Researcher with the Group of Waves, Signals, and Systems, Linnaeus University. From 2019 to 2020, she was an Assistant Professor with the Department of Electrical and Information Technology, Lund University, Lund, Sweden. From 2020 to 2024, she was an Assistant Professor with the KTH Royal Institute of Technology. Currently, she is an Associate Professor with the KTH Royal Institute of Technology. She received the Honorary Grant for the Best Graduate of the Year of her M.Sc. Program, in 2011. She is the author of more than 100 scientific publications, including 51 journal articles, and one book. Her research interests include antenna theory, electromagnetic modeling of gold nanoparticles for medical applications, electromagnetic scattering and absorption, inverse problems, electromagnetics of stratified media, double-negative metamaterials, and mathematical physics. She is leading research as a Principal Investigator within her projects, "Waveguide Theory for Artificial Materials and Plasmonics" and "Gold nanoparticles for High-Frequency Deep Brain Stimulation" awarded by the Swedish Research Council, in 2019 and 2023, respectively. She is the Second Youngest Woman Ever to be awarded a Ph.D. degree from KTH Royal Institute of Technology. She has won multiple teaching and research awards, including the L'Oréal-UNESCO For Women in Science Sweden Award, in 2021, and the Göran Gustafsson Prize for Young Researchers in Physics and Mathematics, in 2024.